Available online at www.sciencedirect.com

ScienceDirect

Biomedical Journal

journal homepage: www.elsevier.com/locate/bj

Original Article

# Quantifying cell behaviors in negative-pressure induced monolayer cell movement

Shu-Er Chow [a], Carl Pai-Chu Chen [b], Chih-Chin Hsu [c,d,*], Wen-Chung Tsai [e], Jong-Shyan Wang [f], Ning-Chun Hsu [c]

[a] Department of Nature Science, Center for General Studies, Chang Gung University, Taoyuan, Taiwan
[b] Department of Physical Medicine and Rehabilitation, Chang Gung Memorial Hospital at Taipei, Taipei, Taiwan
[c] Department of Physical Medicine and Rehabilitation, Chang Gung Memorial Hospital at Keelung, Keelung, Taiwan
[d] School of Traditional Chinese Medicine, College of Medicine, Chang Gung University, Taoyuan, Taiwan
[e] Department of Physical Medicine and Rehabilitation, Chang Gung Memorial Hospital at Linkou, Taoyuan, Taiwan
[f] Institute of Rehabilitation Science, College of Medicine, Chang Gung University, Taoyuan, Taiwan

ARTICLE INFO

*Article history:*
Received 12 April 2015
Accepted 17 August 2015
Available online 28 March 2016

*Keywords:*
Cell movement
Cytoskeleton
Intercellular junctions
Negative-pressure wound therapy
Wound healing

ABSTRACT

*Background:* Negative-pressure of 125 mmHg (NP) has been shown to accelerate wound healing. Effects of NP on human keratinocyte behaviors during wound healing process were highlighted in this study.

*Methods:* An NP incubator incorporating the electric cell–substrate impedance sensing (ECIS) technique has been built to quantify monolayer keratinocytes movement in serum-free media at the ambient pressure (AP) and NP for 12 h. Monolayer cell motions were continuously recorded by ECIS in the frequency range of 22.5–64 kHz. Membrane capacitance ($C_m$), cell–substratum resistance ($\alpha$), and cell–cell junction resistance ($R_b$) were evaluated in cells at the different pressures.

*Results:* A greater monolayer cell migration distance was found in cells at NP. Decreased cell–substratum adhesion reflected in the significantly low $\alpha$ (AP:NP = ~5 $\Omega^{0.5}$:~3 $\Omega^{0.5}$·cm), decreased integrin expression, and increased cell–substratum distance were seen in cells at NP. A significantly increased $C_m$ (AP:NP = ~4:~8 $\mu F/cm^2$) in association with increased membrane ruffling and microtubule filaments were observed early in the monolayer cell movement at NP. A progressive drop in the $R_b$ from 1.2 $\Omega \cdot cm^2$ to 0.8 $\Omega \cdot cm^2$ corresponding to the gradually decreased E-cadherin expressions were observed 6 h after wound closure after NP treatment.

*Conclusion:* A quick membrane ruffling formation, an early cell–substratum separation, and an ensuing decrease in the cellular interaction occur in cells at NP. These specific monolayer cell behaviors at NP have been quantified and possibly accelerate wound healing.

* *Corresponding author*. Department of Physical Medicine and Rehabilitation, Chang Gung Memorial Hospital at Keelung, 222, Maijin Rd., Keelung, Taiwan. Tel.: +886 2 24329292 ext. 2725; fax: +886 2 27933328.
E-mail address: steele0618@gmail.com (C.-C. Hsu).

Peer review under responsibility of Chang Gung University.
http://dx.doi.org/10.1016/j.bj.2015.08.005

## At a glance commentary

### *Scientific background on the subject*

We have scientifically documented morphological adaptations, including increased membrane ruffling, increased cell–substratum separation, and decreased cell–cell adhesion, in keratinocytes at a negative-pressure of 125 mmHg (NP). Cytoskeleton re-organizations, altered adherens junction, and integrin proteins may play important roles in NP-induced accelerated wound healing process.

### *What this study adds to the field*

We have established a wound healing model with better $O_2$ and $CO_2$ tension controls for observing cell behaviors at NP. The results will contribute to the understanding of cell behaviors in NP, aid in refining the contemporary treatment modality, and encourage the development of new facilities in the future.

Changing environmental pressures have been applied to preserve food and treat human diseases in modern science. Hypobaric storage significantly inhibits the respiratory intensity and extends the storage life by up to 50 days for green asparagus [1]. Hyperbaric oxygen (HBO) therapy is defined as a treatment in which patients intermittently breathe 100% oxygen in a chamber of the pressure greater than sea level and is widely accepted as the treatment of chronic wounds [2]. In endothelial cells at the HBO environment for 5 h, 19 genes involved in adhesion, angiogenesis, inflammation, and oxidative stress were down-regulated, and only angiogenin gene expression was up-regulated [3].

In contrast to HBO therapy, negative-pressure wound therapy (NPWT), creating a negative-pressure gradient of 125 mmHg (NP) to accelerate wound healing, has gained popularity in current wound cares [4]. Basic sciences for this therapy have been proposed as creating a moist wound healing environment, enhancing angiogenesis at the wound bed, and reducing bacterial loads [5]. Decreased E-cadherin expression and enhanced cell locomotion have also been shown in several studies [5–9]. Although, all of the above studies have provided valuable information on the effects of NP on wound healing at tissue, cell, and even molecular levels, they have reported the end results rather than a process of the group cells migration.

Cutaneous wound healing is a dynamic biological process involved in keratinocytes re-epithelialization which is majorly associated with migration of keratinocytes at the wound edge. Keratinocytes migrate both individually and as a cellular sheet over the denuded dermis to form a new epidermis [10]. Therefore, keratinocytes become the target in the study. Monolayer cell movement, which refers to two or more cells moving together coupled by cell–cell junctions, is a well-orchestrated multi-steps process that is involved in cutaneous wound healing [11]. The cell group behavior retains a single cell migration cycle, including protrusions of the cell leading edge and disassembly of the cell rear adhesion, and preserve intercellular adhesions [12]. A monolayer epithelial cell model for cell locomotion in wound healing has shown that the force of the lamellipodia, the cell–stratum attachment, and the cell–cell adhesion are the primary interactions governing the monolayer movement [13]. The results were derived by the serial time-lapse images instead of uninterrupted recordings of cell layers at ambient pressure (AP). To observe cell movement of wounded keratinocytes in NPWT, an investigation which is capable of continuously monitoring monolayer cell movement without interruption of the applied NP is indicated.

Electric cell–substrate impedance sensing (ECIS) is a method of obtaining information regarding changes in cell motions and of cell morphology. The cell motion can be continuously recorded with high reproducibility and the resolution order for the cell motion is nanometers [14]. Cell parameters such as cell–substratum resistance ($\alpha$), transmembrane capacitance ($C_m$), and intercellular resistance ($R_b$) of cell monolayers can be calculated by the developed cell–electrode model [15]. The doubling time of HaCaT cells is 21 h [16]. In order to focus on cell movement and eliminate the cell proliferation confounding factor, cells were treated with different pressures for 12 h [5]. Thus, effects of NP on cell proliferation can be neglected for the healing model of wounded monolayer keratinocytes in the study. Our hypothesis in this study was that compared with cells at AP, cells at NP for 12 h would display reduced cell–substratum, and cell–cell adhesions with a significant cell deformation. Quantification of cell behaviors at NP for 12 h is indicated to testify this hypothesis. The results will contribute to the understanding of cell behaviors in NP, aid in refining the contemporary treatment modality, and encourage the development of new facilities in the future.

## Materials and methods

### *Cell culture*

Human skin keratinocytes (HaCaT cell line), kindly provided by Dr. Weng-Hung Chung (Department of Dermatology, Chang Gung Memorial Hospital, Linkou, Taiwan), were cultured in DMEM/F12 (Sigma–Aldrich Corporation, St. Louis, MO, USA) containing 10% fetal bovine serum (FBS) and 100 μg/mL streptomycin–penicillin.

### *Cell viability*

Keratinocytes ($3 \times 10^4$) were seeded in each well of two different eight-well cell culture clusters (Corning Incorporated, Corning, NY, USA) and were incubated in DMEM/F12 solution with 10% FBS overnight. The attached cells were then respectively placed at AP and the NP in a NPI (NPI1500, Linston Advanced Technology Corporation, Longtan, Taoyuan, Taiwan, China) for 12 h. The cells were washed with phosphate buffer saline (PBS) for 5 times to simulate the serum-free condition and were then incubated at AP and NP for 12 h. The relative cell viability (%) related to the cells incubated with 10% FBS at AP was calculated ($n = 8$ in each condition) as our previous protocol [5].

### *Measurement of monolayer cell migration at ambient pressure and negative-pressure*

Cells ($2 \times 10^6$) in serum-free media were seeded on each 35-mm culture dish (Corning Incorporated). A pipette tip (0.1–10 μl, Labcon North America, Petaluma, CA, USA) was used to create a scratch wound in eight culture dishes. They were respectively incubated at AP ($n = 4$) and NP ($n = 4$) for 12 h. The scratched wound size was measured immediately and 12 h after wounding in the two different pressures. The difference between the initial distance and that after 12 h of incubation was defined as the migration distance [Fig. 1].

### *Cell behaviors quantified by the electric cell–substrate impedance sensing technique*

Cells were added to each well of an 8W1E electrode array (Applied Biophysics, Troy, NY, USA) according to our previous procedure [5,8]. Electrical activities were continuously recorded for 12 h while cells becoming confluent at the two different pressures. We measured the impedance for both a cell-free electrode and the same electrode with cells at frequencies that ranged from 22.5 Hz to 64 kHz with the ECIS (1600R, Applied Biophysics, Troy, NY, USA) [17]. The data taking and curve fitting from model calculation are same as those described previously, and the α ($\Omega^{0.5}\cdot$cm), $R_b$ ($\Omega\cdot cm^2$), and $C_m$ (μF/cm$^2$) in monolayer cells were derived from the following mathematical models [14,15,17,18].

$$\alpha = r_c\sqrt{\frac{\rho}{h}} \tag{1}$$

$$\frac{1}{Z_c} = \frac{1}{Z_n}\left\{\frac{Z_n}{Z_n + Z_m} + \frac{\frac{Z_m}{Z_n+Z_m}}{\frac{\gamma r_c}{2}\frac{I_0}{I_1} + R_b\left(\frac{1}{Z_n}+\frac{1}{Z_m}\right)}\right\} \tag{2}$$

$$Z_m = 2\left[\left(\frac{1}{R_m}\right) + (kfC_m)\right]^{-1} \tag{3}$$

where, ρ ($\Omega\cdot$cm) is resistivity of the cell culture medium, h (nm) is an average separation between the ventral cell surface and the substrate, and $r_c$ (μm) is cell radius. The $R_b$ is cell–cell junction resistance between adjacent cells over a unit area and can be obtained from the Equation (2). The $Z_c$ ($\Omega\cdot cm^2$) is specific unit area impedance of the cell-covered electrode, $Z_n$ ($\Omega\cdot cm^2$) is specific impedance of the cell-free electrode, $Z_m$ ($\Omega\cdot cm^2$) is specific impedance through both ventral and dorsal cell membranes, and $I_0$ and $I_1$ are modified Bessel functions of the first kind of order 0 and 1. The $C_m$ can be derived from the resistance of the cell membrane ($R_m$), the alternating current frequency (f), the constant k, and the $Z_m$.

These values were obtained in the confluent layer and at every one-hour interval after confluent layer formation for 12 h at the two different pressures.

### *Protein analysis*

Keratinocytes ($2 \times 10^6$) were seeded in 10-cm culture dishes ($n = 6$) and were then incubated overnight at AP. Three dishes of cells were incubated at each of the two different pressures for 12 h and were then detached by 1% trypsin. Cell pellets from three dishes in each pressure condition were treated with the Q proteome cell compartment kit (Qiagen Sciences, Inc., Germantown, MD, USA). The kit sequentially extracted proteins in cytosols, membranes, nucleus, and cytoskeletons. Each fraction protein of 20 μg was separated by using a 10% sodium dodecyl sulfate–polyacrylamide gel and was transferred to polyvinylidene difluoride membranes (Immobilon (TM)-P, Millipore, Bedford, MA, USA). Processed samples were incubated overnight with primary rabbit monoclonal anti-β-catenin (Cell Signaling Technology Inc., Boston, MA, USA) antibodies. The other treated cells at AP and NP ($n = 15$ in each pressure) for 0 h, 3 h, 6 h, 9 h, and 12 h ($n = 3$ in each time interval) were scraped off the substratum. The primary rabbit monoclonal anti-E-cadherin antibody (Cell Signaling Technology Inc., Boston, MA, USA) was used to determine E-cadherin expressions in the total cell lysate. Primary rabbit monoclonal anti-integrin α4, anti-integrin β1, and anti-integrin

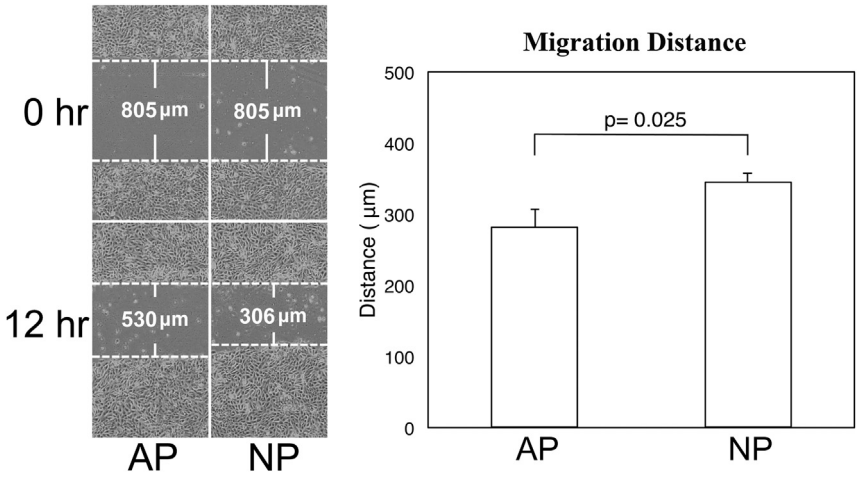


Fig. 1 – The difference in the scratched wound distance between the status immediately post wounding (0 h) and that after 12 h of incubation at the two different pressures was defined as the migration distance (n = 4 in each pressure condition). A significantly greater migration distance was observed in cells at negative-pressure for 12 h.

β4 (Cell Signaling Technology Inc., Boston, MA, USA) were also used to analyze total cell lysates at AP and NP for 12 h.

The mouse monoclonal anti-glyceraldehyde-3-phosphate dehydrogenase, anti-tubulin, and anti-lamin antibodies (Cell Signaling Technology Inc., Boston, MA, USA) were used as the internal reference for cytoplasmic, cytoskeleton, and nuclear proteins, respectively. The mouse monoclonal anti-$Na^+/K^+$ $ATP_{ase}$ (Santa Cruz Biotechnology Inc., Dallas, TX, USA) was used as the reference for a membrane protein. Secondary anti-rabbit or anti-mouse HRP-conjugated IgG antibodies were then added for at least 1 h. The immunoreactive protein bands were visualized using enhanced chemiluminescence (ECL®, Amersham Pharmacia Biotech, Freiburg, Germany). The protein amounts were measured using ImageJ Version 1.440 (National Institutes of Health, USA) [5].

### *Scanning electron microscopic examination*

Cells at AP and NP in serum-free DMEM/F12 medium for 12 h were fixed in 3% glutaraldehyde in a 0.1 M sodium cacodylate buffer (pH = 7.4) for 12 h at 4 °C. They were rinsed with 0.2 M sodium cacodylate for one hour. Following postfixation in 1% osmium tetroxide for 30 min, cells were dehydrated through graded ethanol and were coated with 200 nm gold by an utter coater (Balzers Union SCD 050 apparatus, BAL-TEC, PA, USA). The processed samples were then examined with a scanning electron microscopy at 15 kv (S5000, Hitachi High Technologies America, Inc., Schaumburg, IL, USA) in the frontal and sagittal planes.

### *Fluorescent stain*

Cells ($10^5$) were inoculated in each well of the eight-chamber slide (Millicell EZ slide, Millipore Corp., Billerica, MA, USA) and were incubated at the two different pressures serially for 0 h, 3 h, 6 h, 9 h, and 12 h. A pipette tip was used to create a scratch wound in each well. The cells were stained with primary rabbit monoclonal anti-E-cadherin, anti-β-catenin, and anti-acetylated α-tubulin antibodies (Cell Signaling Technology Inc., Boston, MA, USA). Fluorescein isothiocyanate-conjugated AffiniPure Goat anti-rabbit IgG (Jackson ImmunoResearch Laboratories, West Grove, PA, USA) was used as the secondary antibody. Nuclei were counterstained with mounting medium (Vector Laboratories Inc., Burlingame, CA, USA) containing 4′,6-diamidino-2-phenylindole. The stained cells were examined with a confocal microscopic examination at a magnification of ×1000 (Leica TCS SP2, Leica Microsystems Inc., Buffalo Grove, IL, USA).

### *Luciferase assay*

To detect β-catenin response elements (RE) activities in AP- or NP-treated cells ($n$ = 3 in each condition), transfections of

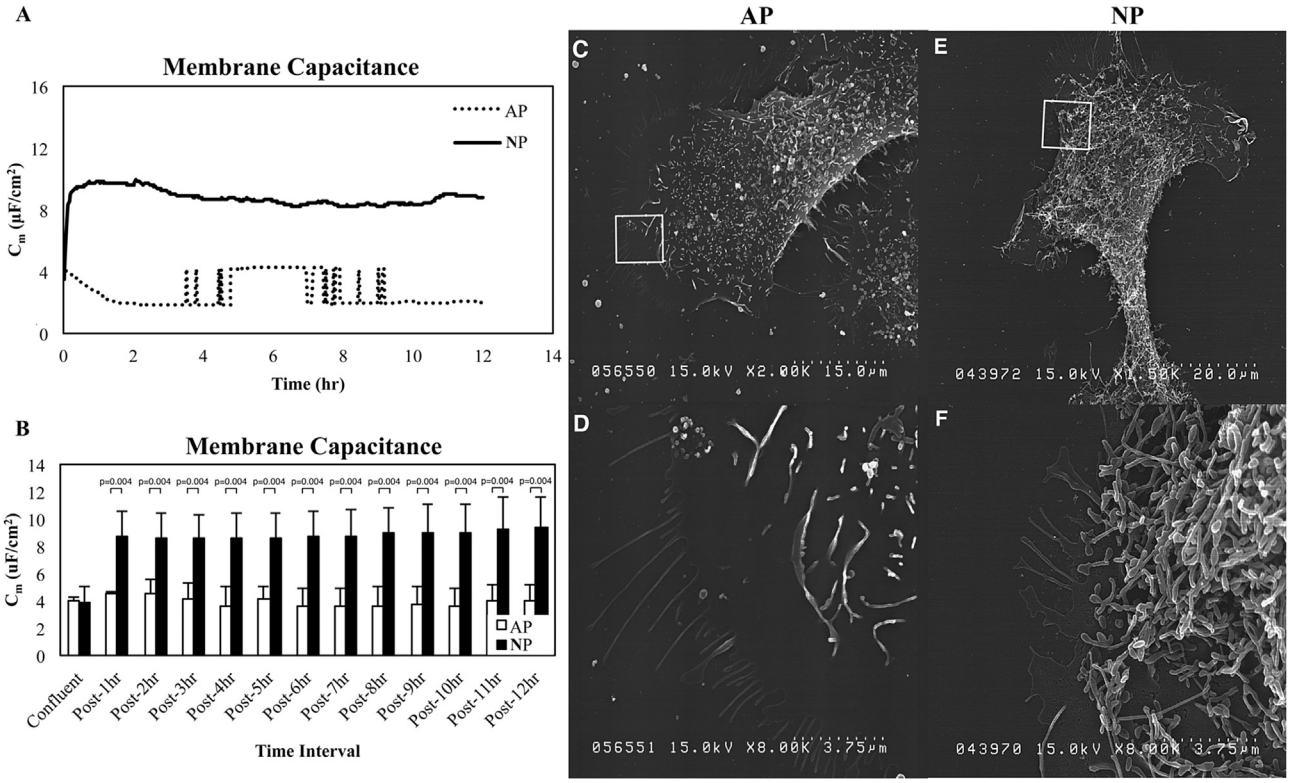


Fig. 2 – (A) The membrane capacitance ($C_m$) was continuously recorded for 12 h starting from cells becoming confluent at ambient pressure (·····) and negative-pressure (—). The $C_m$ increased quickly in cells at negative-pressure, whereas the value was relatively stable in cells at ambient pressure. (B) The capacitance maintained constantly during the 12 h recording period at ambient pressure. A significant increase in $C_m$ (8 μF/cm²) was observed in cells at negative-pressure during the recording period. (C and D) scanning electronic microscopic images for keratinocytes in 2K and 8K magnifications. In comparison with cells at ambient pressure, (E and F) distinct membrane ruffles were observed in the scanning electronic microscopic images for the cells at negative-pressure.

luciferase reporter plasmids, and pSV-β-galactosidase control vector (Promega Corp., Madison, WI, USA) were performed using Lipofectamine 2000 (Invitrogen, Carlsbad, CA, USA). After incubation for 6–12 h, the cells were rinsed with PBS and were lysed in 100 μl of reporter lysis buffer (Promega Corp., Madison, WI, USA). The mean normalized luciferase activity was taken [19].

### Statistical analysis

The Mann–Whitney U-test was used to assess the cell migration distance, cell behaviors, including $\alpha$, $C_m$, and $R_b$, E-cadherin expressions, β-catenin expressions, and β-catenin activity between cells at AP and NP. A $p < 0.05$ was considered statistically significant.

## Results

### Negative-pressure enhancing monolayer cell migration

Relative cell viability of those with FBS at NP was 105% ± 6.5%. The viability in those cultured in serum-free medium at AP and NP was approximately 90%. An average wound gap of 1.0 ± 0.3 mm was created on cell monolayer in each well. A significantly ($p = 0.025$) greater migration distance of 346 ± 12 μm was observed in cells at NP ($n = 4$) compared with 282 ± 25 μm at AP ($n = 4$) [Fig. 1].

### Immediate cell deformation at negative-pressure

The $C_m$ of an intact monolayer was approximately 4 μF/cm$^2$ which was maintained constantly during the 12 h post-confluent period at AP. The $C_m$ increased immediately and significantly ($p < 0.05$) from 4 μF/cm$^2$ to 8 μF/cm$^2$ in cells at NP within 1 h [Fig. 2A and B]. In comparison with cells at AP [Fig. 2C and D], distinct membrane ruffles were observed in cells at NP on scanning electron microscopic (SEM) images [Fig. 2E and F].

### Negative-pressure release cell–substratum adhesion

The $\alpha$ value maintained at approximately 5 $\Omega^{0.5}$·cm during the recording period in cells at AP. However, the $\alpha$ decreased progressively from 5 $\Omega^{0.5}$·cm to 3 $\Omega^{0.5}$·cm at NP [Fig. 3A]. Differences in the $\alpha$ values between AP and NP were significant at each recording point [Fig. 3B]. The SEM images also demonstrated the tendency of having a greater cell–substratum distance (h) in cells at NP than those at AP [Fig. 3C–F]. The h can be estimated according to the previous developed model and the assumed HaCaT cell radius of 12 μm [8]. Therefore, the

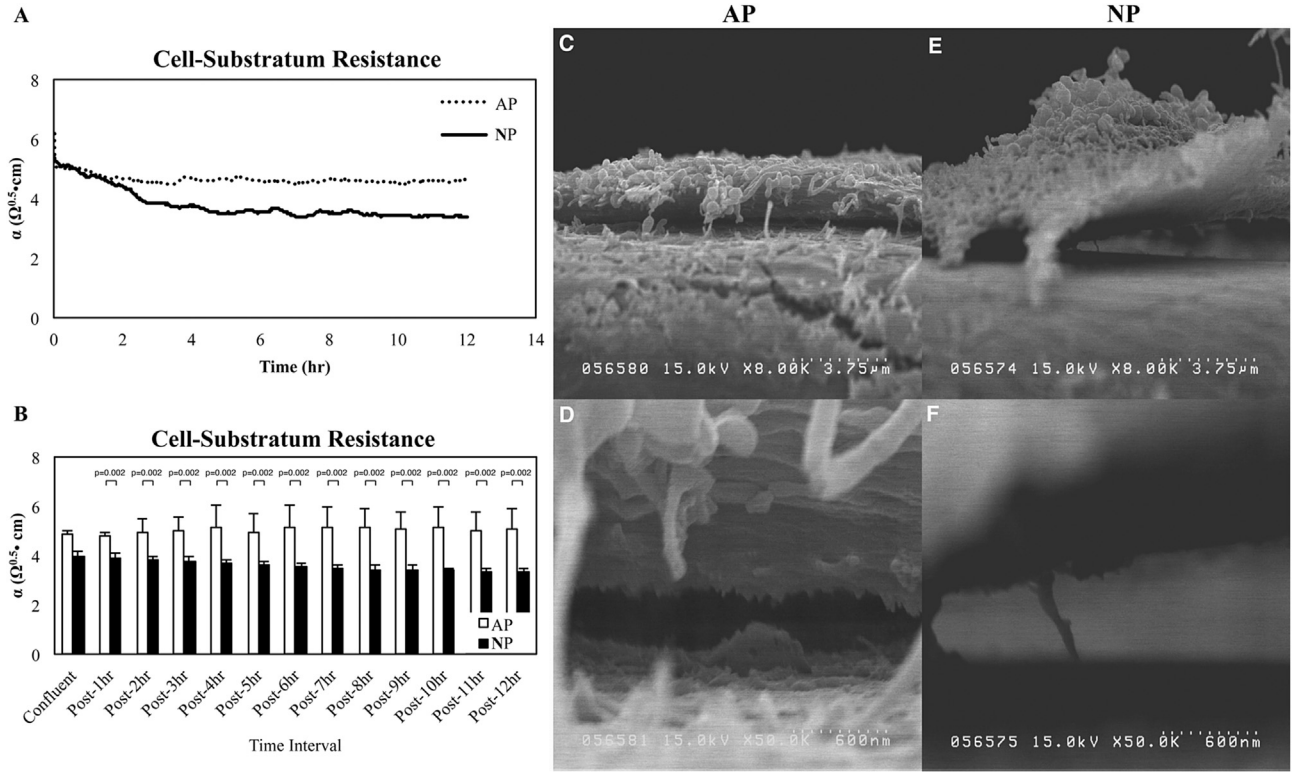


Fig. 3 – (A) The cell–substratum resistance ($\alpha$) was continuously measured starting from cells becoming confluent at ambient pressure (·····) and negative-pressure (—). The resistance decreased progressively in cells at negative-pressure, however, the level kept constant in cells at ambient pressure. (B) The average $\alpha$ value at the confluent monolayer, and every 1 h interval post confluent layer formation for 12 h at the two different pressures were recorded. A significant decrease of $\alpha$ was observed in cells at negative-pressure. (C–F) scanning electronic microscopic images for the cell–substratum distance at 8K and 50K magnifications showed increased cell–substratum separation in cells at negative-pressure (>600 nm). The separation in cells at ambient pressure was 140–400 nm.

estimated h in confluent monolayer was approximately 120 nm. A significant difference ($p = 0.024$) in the h at the 12th h after cells becoming confluent between AP (109 ± 17 nm) and NP (229 ± 95 nm) was observed. A significant ($p = 0.02$) decrease of integrin α4 was observed in cells at NP. However, expressions of integrin β1 and β4 did not change in cells at NP [Fig. 4].

### *Negative-pressure weakening cell–cell junctions*

The $R_b$ represents the monolayer barrier function and was shown in Fig. 5A [13]. The $R_b$ in confluent cell layer was approximately 1 Ω $cm^2$. However, the barrier function decreased progressively in cells at NP, and significant changes ($p < 0.05$) were observed 6 h after cells becoming confluent [Fig. 5B]. The $R_b$ 12 h after the formation of an intact cell layer was 1.2 Ω·$cm^2$ and 0.8 Ω·$cm^2$ at AP and NP, respectively. Evidences concerning sequential cell–cell junction protein expressions support the above findings. The E-cadherin expressions remained similar in cells at the both pressures for <12 h and significantly decreased ($p = 0.016$) in cells at NP for 12 h [Fig. 6].

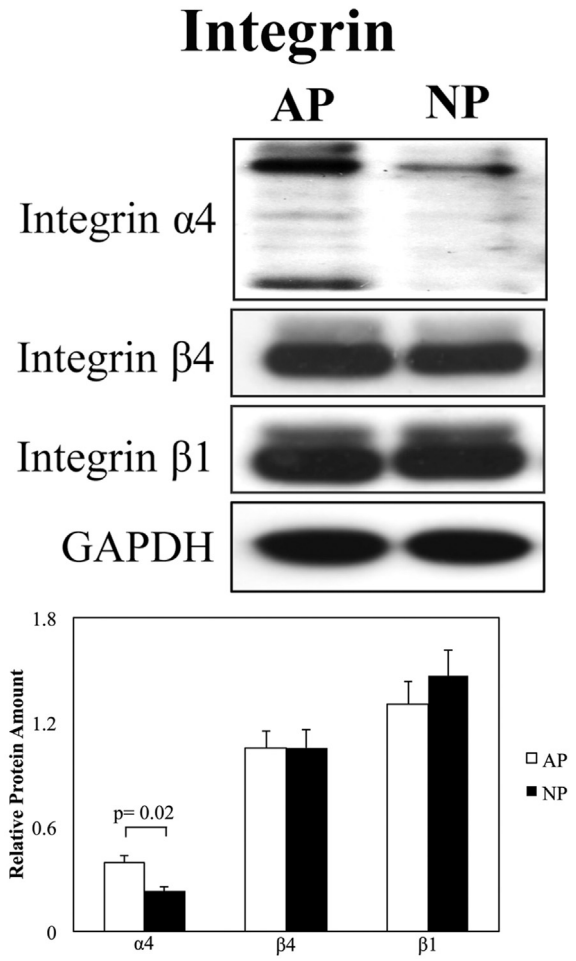


Fig. 4 – A significant decrease ($p = 0.02$) of integrin α4 expression was observed in cell at negative-pressure for 12 h, while compared with those at ambient pressure for 12 h. The levels of integrin β1 and 4 were similar in cells at ambient pressure and negative-pressure, respectively.

### *Sequential images for cell spreading and cell–cell junctions*

Thick and long acetylated α-tubulin filaments were observed in cells at NP early in the wound healing process. β-catenin expression decreased in cells at NP for longer than 6 h. However, increased β-catenin expression in the cytosols and nuclei of cells at NP were observed as early as 3 h during the cell layer movement [Fig. 7].

### *Negative-pressure enhancing the translocation of β-catenin from the plasma membrane to the nucleus*

Protein analysis for β-catenin in different cell fractions showed a tendency of nuclear localization of β-catenin during the wound healing process. The proportion (protein amount in each fraction/total protein amount) of β-catenin was used to show the distribution of β-catenin in different cell fractions. The β-catenin expression significantly decreased ($p = 0.029$) in the plasma membrane but significantly increased ($p = 0.01$) in the nucleus at NP [Fig. 8]. To study the NP-induced transcriptional regulation of the putative β-catenin RE, the cells were transfected with a pGL3-β-catenin-RE-Luc vector that

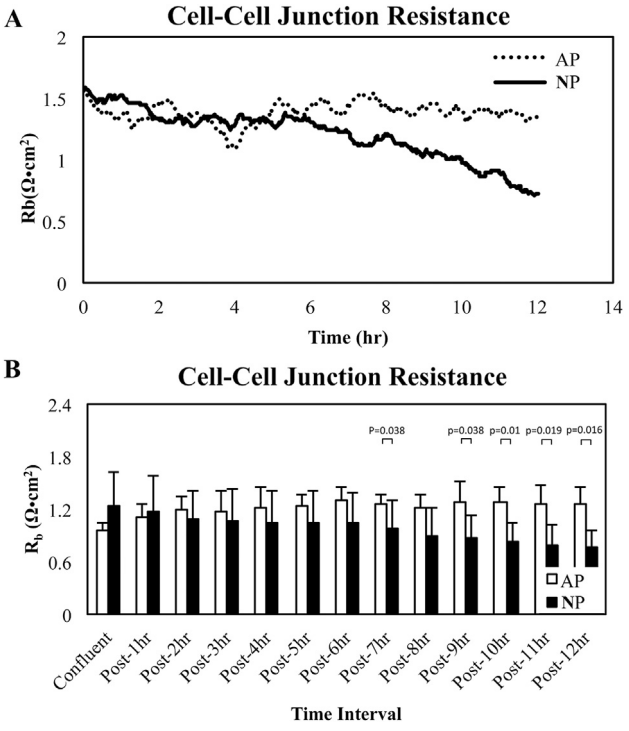


Fig. 5 – (A) The intercellular resistance ($R_b$) was continuously recorded starting from cells becoming confluent at ambient pressure (·····) and negative-pressure (—). In comparison with cells at ambient pressure, the intercellular resistance maintained constantly and decreased progressively in cells treated with negative-pressure longer than 6 h. (B) The confluent layer $R_b$ was approximately 1–1.2 Ω·$cm^2$ the barrier function decreased progressively in cells at negative-pressure and significant changes ($p < 0.05$) were observed 6 h after negative-pressure treatment. The $R_b$ in cells at negative-pressure decreased from 1.2 Ω·$cm^2$ to 0.8 Ω·$cm^2$ while the value was relatively stable in cells at ambient pressure.

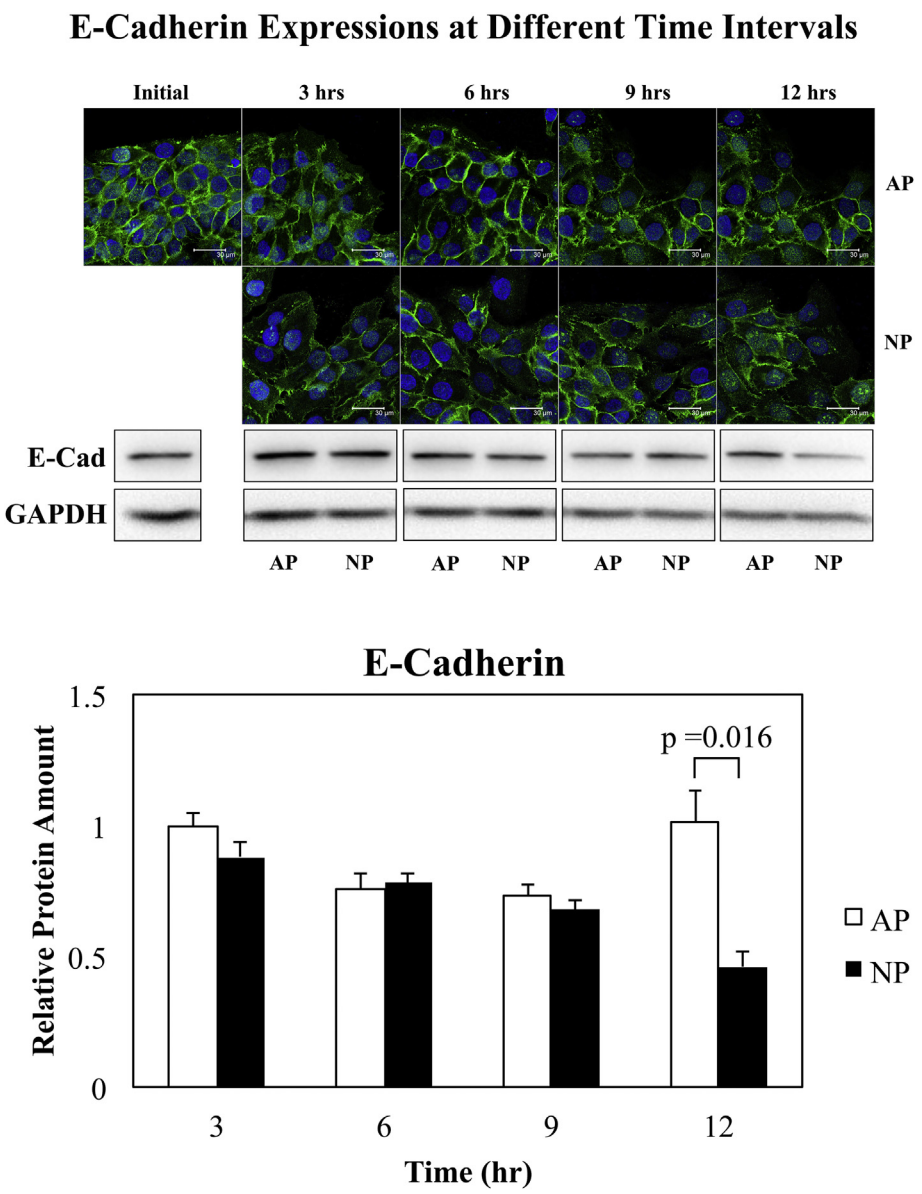


Fig. 6 – The E-cadherin expression relative to the initial amount (0) was similar in the 3 h, 6 h, and 9 h at both pressures. However, a trend of decrease in E-cadherin expression was observed in cells at negative-pressure for 12 h. Cells at negative-pressure 12 h after wounding had obviously decreased E-cadherin expression in fluorescent strains (×400).

contained five copies of a β-catenin-RE followed by a minimal TATA box and a luciferase gene. When given NP treatment for 6 h, the cells significantly ($p = 0.02$) elicited a greater than ~1.3-fold stimulation of the reporter activity compared with the AP. With the NP treatment for 12 h, the cells elicited a significantly ($p = 0.02$) greater than ~1.6-fold stimulation of the reporter activity compared with at AP [Fig. 9].

## Discussion

The confluent monolayer cell activities can reflect what occurs before the wound healing process because the wound healing process is a continuous cell behavior. In contrast to other previous spontaneous cell layer motion models obtained by intermittent captured images [13,20,21], cell behaviors have been obtained by continuously recording cell electrical activities at externally applied NP. Cell migration instead of proliferation activity was not remarkable in cells at AP and NP for 12 h in our previous observation [5]. NP accelerated collective keratinocyte migration in the traditional wound healing assay, and the finding resembled the quick epithelial wound healing measured at NP using electric wound healing assay [5,8]. It is believed that enhanced collective cell migration is a dominant physiological adaptation in the first 12 h of keratinocytes at NP.

A typical $C_m$ recording for confluent keratinocytes showed an approximate capacitance of 4 μF/cm$^2$. The short time interval between the peak $C_m$ and the stable status reflects the quick cell adaptations at NP [8]. Deformation of the cells at NP, including enlarged dimensions, decreased thickness, and

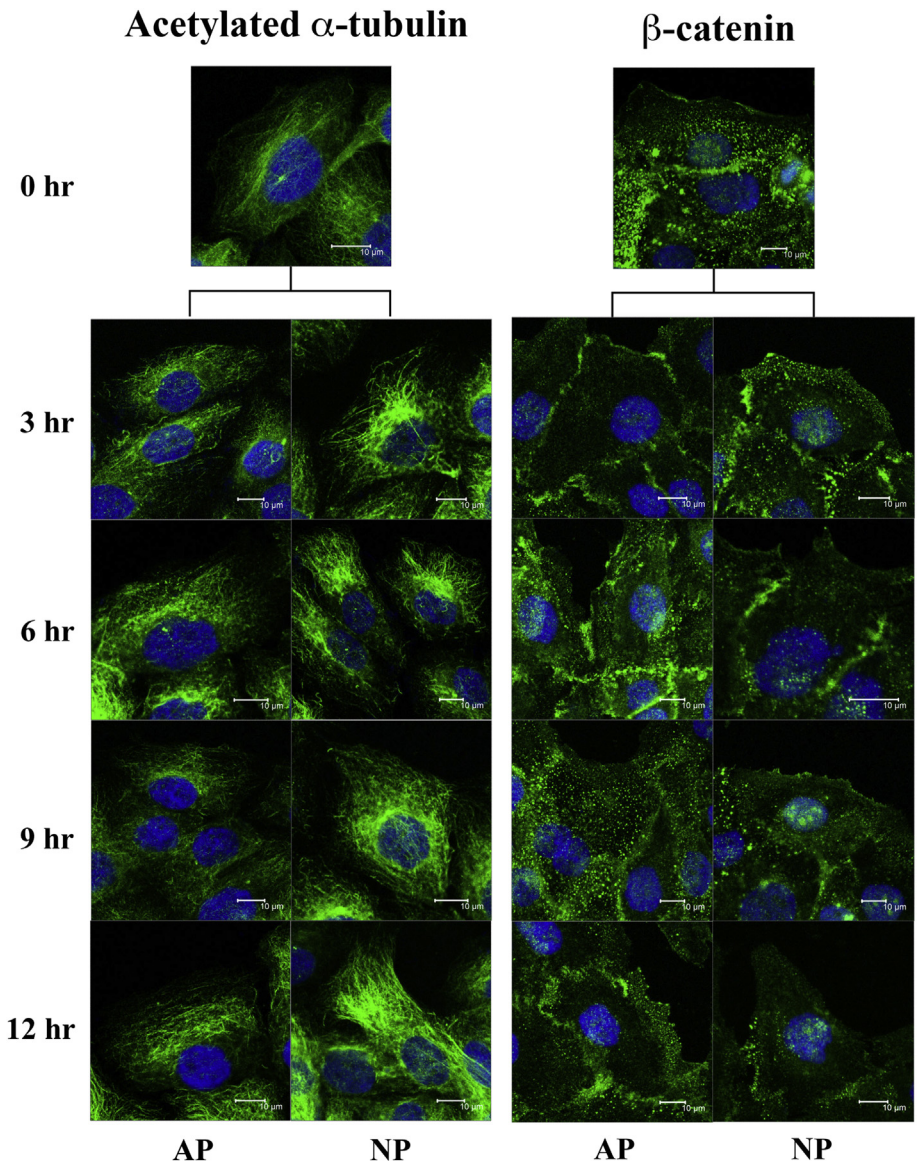


Fig. 7 – Fluorescent stains of acetylated α-tubulins (left panel) in cells at 0 h, 3 h, 6 h, 9 h, and 12 h after creating a scratched wound in the monolayer cells. Thick and long microtubule filaments have been observed since 3 h after wounding in cells at negative-pressure (×1000). Serial images for β-catenin at 0 h, 3 h, 6 h, 9 h, and 12 h (right panel) after injury to the monolayer cell. The β-catenin expressions on membranes were similar in cells at ambient pressure and negative-pressure in the first 6 h post injury period. A remarkable decrease in the protein expressions was observed in cells at negative-pressure for longer than 6 h. Increased β-catenin expressions were observed in the nucleus of the cells at negative-pressure.

extruding cell fronts has been reported [5]. The SEM images in the study showed additionally increased dorsal membrane ruffling in cells at NP. Thick and long acetylated α-tubulin filaments were observed in cells at NP in our serial fluorescent stains at the early cell layer migration stage. The acetylated α-tubulin is considered to represent the subpopulation of more stable microtubules in the cell [22]. Involvement of the cytoskeleton re-organization could causes an increase in the cell membrane surface area and in turn results in persistently greater membrane capacitance in cells at NP.

The $\alpha^2$ ($\Omega \cdot cm^2$) has been reported to be inversely proportional to the average cell–substratum separation [14,23]. The lower the value of $\alpha$ is the weaker the cell–substrate adhesion [17]. The decreased $\alpha$ in a confluent monolayer at NP can be related to changes in cell–substratum adhesion. The resistance at NP was persistently less than that at AP and this finding resulted from the increased cell–substratum distance in cells at NP (~230 nm in NP vs. ~110 nm in AP) for 12 h. Sagittal SEM images of cells at NP had a greater cell–substratum distance than those of cells at AP. The integrin α4-paxillin complex inhibits stable lamellipodia, thus confining lamellipodia formation to the cell front [24]. Decreased integrin α4 expressions in cells at NP may reflect the weak cell-substratum adhesion and remove the inhibition

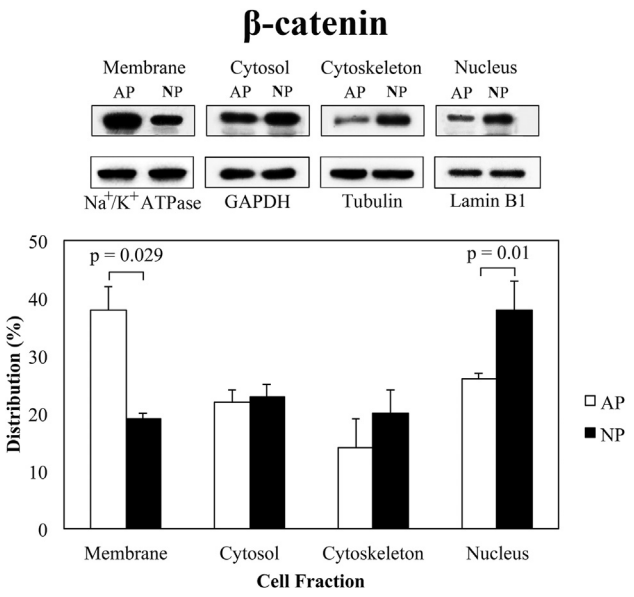


Fig. 8 – Analysis of β-catenin in different cell fractions, including the plasma membrane, cytosol, cytoskeleton, and nucleus, of cells at ambient pressure and negative-pressure for 12 h. Findings that concerned the β-catenin distribution portions were different between the cells at ambient pressure and negative-pressure. Significantly decreased membrane bound β-catenin was observed in cells at negative-pressure. A significant increase of β-catenin distribution in the nucleus was also found in cells at negative-pressure.

of Rac activities. These findings can accelerate the monolayer cell movement.

The intercellular resistance maintained at a constant level in cells at AP, whereas the value kept decreasing in those at

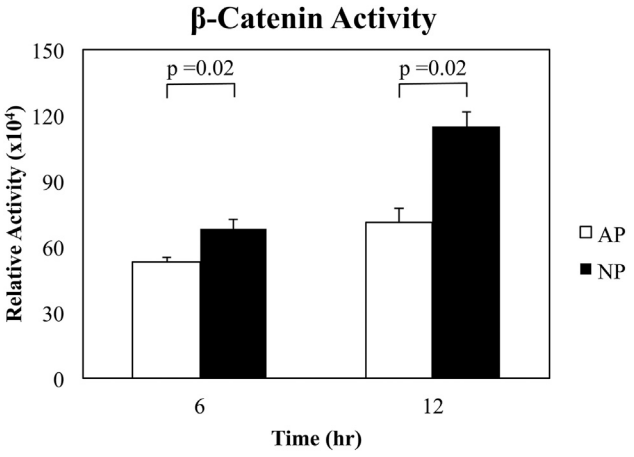


Fig. 9 – Cells were transfected with a pGL3-β-catenin-RE-Luc vector to study the negative-pressure induced transcriptional regulation of the putative β-catenin response. The cells at negative-pressure for 6 h elicited a greater (~1.3-fold) stimulation of the reporter activity than that at ambient pressure. With negative-pressure treatment for 12 h, the cells also elicited a greater (~1.6-fold) stimulation of the reporter activity compared with that at ambient pressure.

NP. A significant decrease ($p < 0.05$) in $R_b$ was observed after NP treatment for longer than 6 h [Fig. 5]. Western blot results showed a decrease trend of relative E-cadherin amount in cells at NP longer than 6 h, but only those treated for 12 h had a significant decrease ($p = 0.016$) of relative E-cadherin amount. Gel loading and transfer from gel to the membrane can introduce error during Western blotting. Small amounts of protein may transfer inefficiently. The above technique errors may result in the variance between the protein analysis and the cell electrical activity measurements [25]. Translocation of β-catenin protein from the plasma membrane to the nucleus functions as an activator involving in adherens junction dynamics, tissue morphogenesis and cell migration [26]. Serial fluorescent stains for β-catenin have demonstrated that this protein expression decreased in the plasma membrane but increased in the nucleus during the 12 h treatment at NP [Fig. 7]. A significant decrease of membrane bound β-catenin and a significant increase of nuclear localization of β-catenin at NP corresponded with the cell fluorescence expression [Fig. 8]. Increased β-catenin activity has been noticed in cells at NP [Fig. 9]. It is believed that NP can induce the translocation of β-catenin from the membrane to the nucleus. This protein movement may in turn facilitate cell locomotion.

Cells at the wound leading edge are prone to move toward the low cell density area based on the mechanisms of contact inhibition of locomotion [27]. Traction forces are driving a cell layer motion not only arise predominately in leader cells but also arise in many cell rows that are behind the leading edge and extend across enormous distances [21]. This arrangement allows a monolayer to migrate directionally toward the free space, to produce efficient wound closure. E-cadherins have long been key suspects in the force transmission [28]. In our study, E-cadherins decreased late at NP, and the existence of the intercellular junction protein is beneficial for directed monolayer cell migration. Leading edge cells move further into the low cell density area and result in the decrease of cell junction protein expressions. In this study, we have focused on cell behaviors of cell adhesion, cell ruffling, and intercellular resistance at NP with the cell model. The NP-induced signal transduction has not been clarified. Future *in vivo* experiment in Sprague–Dawley rats for the physiological adaptation in different wound cells at NP, the NP applied length, and wound size effects will be performed.

## *Conclusion*

Electrical activities for the cell layer movement at NP reveal a significant increase in the membrane capacitance initially following a significant decrease in the cell–substratum resistance. Although, cell junction protein expressions do not decrease until 6 h of NP treatment, translocations of β-catenin to the nucleus in the early NP treatment phase. During the first 6 h of NP treatment, traction forces that are produced by the NP driving monolayer cell migration because of the existing cell–cell junctions. The cell layer in the front edge moves quickly or even escapes from the following cell rows behind it, to cover the bare area. The progressive decrease in the cell–cell interaction occurs with the continuous applications of NP on the cells for longer than 6 h. Observations in the study demonstrate that quick cytoskeleton re-organizations,

cell–substratum separation, and cell–cell junction loosening play important roles in NP-regulated monolayer cell migration.

## Source of support

Nil.

## Conflicts of interest

The authors declare no conflicts of interest.

## Acknowledgment

We thank the Chang Gung Medical Research Program grants (CMRPG2A0361, CMRPG2B0471, CMRPG2D0031, and CMRPG2C0381) and our National Science Council grant (NSC100-2314-B-182-053-MY3) for support of our academic research. We also appreciate the excellent confocal microscopic images provided by Mr. Hsiao-Tung Liu in Laser Scanning Confocal Microscopic Room, Chang Gung Memorial Hospital, Keelung. Chun-Min Lo in Department of Biomedical Engineering, National Yang-Ming University, Taipei, has help us process the electrical wound healing assay data.

## REFERENCES

[1] Li W, Zhang M, Han-Qing Y. Study on hypobaric storage of green asparagu. J Food Eng 2006;73:225–30.
[2] Gill AL, Bell CN. Hyperbaric oxygen: its uses, mechanisms of action and outcomes. QJM 2004;97:385–95.
[3] Kendall AC, Whatmore JL, Harries LW, Winyard PG, Smerdon GR, Eggleton P. Changes in inflammatory gene expression induced by hyperbaric oxygen treatment in human endothelial cells under chronic wound conditions. Exp Cell Res 2012;318:207–16.
[4] Morykwas MJ, Argenta LC, Shelton-Brown EI, McGuirt W. Vacuum-assisted closure: a new method for wound control and treatment: animal studies and basic foundation. Ann Plast Surg 1997;38:553–62.
[5] Hsu CC, Chow SE, Chen CP, Tsai WC, Wang JS, Yu SY, et al. Negative pressure accelerated monolayer keratinocyte healing involves Cdc42 mediated cell podia formation. J Dermatol Sci 2013;70:196–203.
[6] McNulty AK, Schmidt M, Feeley T, Kieswetter K. Effects of negative pressure wound therapy on fibroblast viability, chemotactic signaling, and proliferation in a provisional wound (fibrin) matrix. Wound Repair Regen 2007;15:838–46.
[7] Baldwin C, Potter M, Clayton E, Irvine L, Dye J. Topical negative pressure stimulates endothelial migration and proliferation: a suggested mechanism for improved integration of Integra. Ann Plast Surg 2009;62:92–6.
[8] Hsu CC, Tsai WC, Chen CP, Lu YM, Wang JS. Effects of negative pressures on epithelial tight junctions and migration in wound healing. Am J Physiol Cell Physiol 2010;299:C528–34.
[9] McNulty AK, Schmidt M, Feeley T, Villanueva P, Kieswetter K. Effects of negative pressure wound therapy on cellular energetics in fibroblasts grown in a provisional wound (fibrin) matrix. Wound Repair Regen 2009;17:192–9.
[10] Santoro MM, Gaudino G. Cellular and molecular facets of keratinocyte reepithelization during wound healing. Exp Cell Res 2005;304:274–86.
[11] Ilina O, Friedl P. Mechanisms of collective cell migration at a glance. J Cell Sci 2009;122(Pt 18):3203–8.
[12] Ridley AJ, Schwartz MA, Burridge K, Firtel RA, Ginsberg MH, Borisy G, et al. Cell migration: integrating signals from front to back. Science 2003;302:1704–9.
[13] Arciero JC, Mi Q, Branca MF, Hackam DJ, Swigon D. Continuum model of collective cell migration in wound healing and colony expansion. Biophys J 2011;100:535–43.
[14] Giaever I, Keese CR. Micromotion of mammalian cells measured electrically. Proc Natl Acad Sci U. S. A 1991;88:7896–900.
[15] Lo CM, Glogauer M, Rossi M, Ferrier J. Cell-substrate separation: effect of applied force and temperature. Eur Biophys J 1998;27:9–17.
[16] Boukamp P, Petrussevska RT, Breitkreutz D, Hornung J, Markham A, Fusenig NE. Normal keratinization in a spontaneously immortalized aneuploid human keratinocyte cell line. J Cell Biol 1988;106:761–71.
[17] Bagnaninchi PO, Drummond N. Real-time label-free monitoring of adipose-derived stem cell differentiation with electric cell-substrate impedance sensing. Proc Natl Acad Sci U. S. A 2011;108:6462–7.
[18] Lo CM, Keese CR, Giaever I. Monitoring motion of confluent cells in tissue culture. Exp Cell Res 1993;204:102–9.
[19] Chu WK, Dai PM, Li HL, Chen JK. Glycogen synthase kinase-3beta regulates DeltaNp63 gene transcription through the beta-catenin signaling pathway. J Cell Biochem 2008;105:447–53.
[20] Poujade M, Grasland-Mongrain E, Hertzog A, Jouanneau J, Chavrier P, Ladoux B, et al. Collective migration of an epithelial monolayer in response to a model wound. Proc Natl Acad Sci U. S. A 2007;104:15988–93.
[21] Trepat X, Wasserman MR, Angelini TE, Millet E, Weitz DA, Butler JP, et al. Physical forces during collective cell migration. Nat Phys 2009;5:426–30.
[22] Sadoul K, Wang J, Diagouraga B, Khochbin S. The tale of protein lysine acetylation in the cytoplasm. J Biomed Biotechnol 2011;2011:970382.
[23] Lo CM, Keese CR, Giaever I. Impedance analysis of MDCK cells measured by electric cell-substrate impedance sensing. Biophys J 1995;69:2800–7.
[24] Nishiya N, Kiosses WB, Han J, Ginsberg MH. An alpha4 integrin-paxillin-Arf-GAP complex restricts rac activation to the leading edge of migrating cells. Nat Cell Biol 2005;7:343–52.
[25] Bhavsar JH, Remmler J, Lobel P. A method to increase efficiency and minimize anomalous electrophoretic transfer in protein blotting. Anal Biochem 1994;221:234–42.
[26] Tian X, Liu Z, Niu B, Zhang J, Tan TK, Lee SR, et al. E-cadherin/ß-catenin complex and the epithelial barrier. J Biomed Biotechnol 2011;2011:567305.
[27] Abercrombie M, Heaysman JE. Observations on the social behaviour of cells in tissue culture. I. Speed of movement of chick heart fibroblasts in relation to their mutual contacts. Exp Cell Res 1953;5:111–31.
[28] Vedula SR, Ravasio A, Lim CT, Ladoux B. Collective cell migration: a mechanistic perspective. Physiol (Bethesda) 2013;28:370–9.